Surface Science xxx (2015) xxx–xxx

Contents lists available at ScienceDirect

Surface Science

journal homepage: www.elsevier.com/locate/susc

Reaction pathways of model compounds of biomass-derived oxygenates on Fe/Ni bimetallic surfaces

Weiting Yu, Jingguang G. Chen *

Department of Chemical Engineering, Columbia University, New York, NY 10027, United States

ARTICLE INFO

Available online xxxx

Keywords:
Bimetallic surfaces
ML Fe/Ni(111) surface
Biomass-derivatives
Furfural
Glycolaldehyde
Acetaldehyde

ABSTRACT

Controlling the activity and selectivity of converting biomass-derivatives to fuels and valuable chemicals is critical for the utilization of biomass feedstocks. There are primarily three classes of non-food competing biomass, cellulose, hemicellulose and lignin. In the current work, glycolaldehyde, furfural and acetaldehyde are studied as model compounds of the three classes of biomass-derivatives. Monometallic Ni(111) and monolayer (ML) Fe/Ni(111) bimetallic surfaces are studied for the reaction pathways of the three biomass surrogates. The ML Fe/Ni(111) surface is identified as an efficient surface for the conversion of biomass-derivatives from the combined results of density functional theory (DFT) calculations and temperature programmed desorption (TPD) experiments. A correlation is also established between the optimized adsorption geometry and experimental reaction pathways. These results should provide helpful insights in catalyst design for the upgrading and conversion of biomass.

1. Introduction

The declining supply of fossil fuel resources and the increasing energy demand by the rapidly developing economies lead to the imperative development of sustainable energy. Non-food competing biomass, due to its advantages of being abundantly available, renewable and potentially carbon-neutral, is regarded as an alternative energy source to fossil fuels. There are three main classes of non-food competing biomass, which are cellulose, hemicellulose and lignin [1]. It is critical to study the conversion of the three types of biomass resources for the production of valuable chemicals and bio-fuels. However, the low vapor pressure and high molecular weight of large biomass-derivatives bring difficulty into fundamental surface science studies using ultrahigh vacuum (UHV) techniques. Therefore it is important to identify smaller molecules as the model compounds in the surface science study of biomass conversion.

Glucose is produced from cellulose through the hydrolysis process. The key functionalities of glucose are the C – OH and C═O groups. Therefore glycolaldehyde ($HOCH_2CH$═O), the smallest molecule that contains both C – OH and C═O bonds as well as the same C/O ratio as glucose, is selected as a probe compound of cellulosic biomass [2]. Furthermore, according to the literature [3], the contents of glycolaldehyde and aldehydes are as high as 20% in the crude bio-oil from the pyrolysis of lignin biomass. Furfural [4], produced by the hydrolysis and dehydration of hemicellulose, is considered as a model compound of biomass-derivatives from hemicellulosic biomass. Thus, glycolaldehyde, acetaldehyde and furfural are useful surrogate molecules for the reaction pathways of biomass conversion in DFT and UHV surface science studies. One of the reaction pathways for glycolaldehyde and acetaldehyde is the reforming pathway to produce syngas, which can be used in Fischer–Tropsch [5], water gas shift [6,7] and methanol synthesis [8] processes. A desirable conversion pathway of furfural is to produce an important biofuel, 2-methylfuran, through the hydrodeoxygenation (HDO) reaction to remove the oxygen atom in the carbonyl group with the furan ring remaining intact [4].

Previously, as an example of using small alcohols and polyols as the model compounds of biomass, the aqueous-phase reforming of ethylene glycol was compared over different transition metals [9], Pt and Ni were identified as promising monometallic catalysts for the reforming of small oxygenates with both high activity and H_2 selectivity. Bimetallic surfaces and catalysts are known to often exhibit unique properties different from either of the parent metals [10–15] and therefore the Ni/Pt bimetallic catalyst has been extensively studied for small oxygenates. For example, Ni-modified Pt(111) bimetallic surfaces have been studied for the reforming of glycolaldehyde [2], and the monolayer (ML) Ni/Pt(111) surface [16] has been identified to show a higher reforming activity than Ni(111) and Pt(111) monometallic surfaces. However, Pt is expensive and scarce, and therefore non-precious metal Ni(111) is employed to replace Pt(111) as the substrate in the study. Recently, Resasco and the co-workers also studied the furfural reaction on SiO_2-supported Ni [17] and Fe/Ni [18] catalysts. Therefore, in the current study Ni(111) and ML Fe/Ni(111) surfaces are investigated for the reaction pathways of glycolaldehyde, acetaldehyde and furfural molecules via a combination of DFT calculations and temperature programmed desorption (TPD) experiments for the feasibility of using non-precious monometallic and bimetallic surfaces for biomass conversion.

* Corresponding author.
E-mail address: jgchen@columbia.edu (J.G. Chen).

http://dx.doi.org/10.1016/j.susc.2015.01.009
0039-6028/

2. Theoretical and experimental methods

2.1. DFT calculations

All DFT calculations were performed with the Vienna Ab initio Simulation Package (VASP) [19–22] and the PW 91 functional [23] was used in the generalized gradient approximation (GGA) [24] calculation. A kinetic cutoff energy of 396 eV was chosen for the plane wave truncation. All slab calculations were performed with a $3 \times 3 \times 1$ Monkhorst–Pack k-point grid. The clean Ni(111) surface was modeled by adding six equivalent layers of vacuum onto four Ni layers, in which the two bottom layers of the Ni(111) slab were frozen at a metal distance of 2.49 Å, while the top two layers were allowed to relax to reach the lowest energy configuration. The monolayer (ML) Fe/Ni(111) surface was modeled by replacing the Ni atoms in the top layer with Fe atoms. The calculations on Ni(111) and ML Fe/Ni(111) surfaces were performed with spin-polarization. The binding energies of glycolaldehyde, acetaldehyde and furfural were calculated on each surface by subtracting the energies of the bare slab and free molecule from the total energy of the slab plus the corresponding adsorbed molecule. The optimized adsorption configurations of glycolaldehyde, acetaldehyde and furfural on the ML Fe/Ni(111) surface are shown in Fig. 1. A periodic 4×4 unit cell was used in the calculation for furfural to reduce the interaction between the molecules, while a 3×3 unit cell was used for the two smaller molecules. The adsorption coverage is 1/16 (molecule/metal atom) for furfural and 1/9 (molecule/metal atom) for glycolaldehyde and acetaldehyde.

2.2. Surface science experiments

Glycolaldehyde (Fisher scientific, 98%, dimer), acetaldehyde (Sigma-Aldrich, 99.85%) and furfural (Sigma Aldrich, 99%) were transferred into glass sample cylinders separately. Glycolaldehyde was purified using repeated heat-pump-cool cycles, while acetaldehyde and furfural samples were purified using freeze-pump-thaw cycles. All other gases, oxygen, hydrogen, neon, propylene and carbon monoxide were of research purity and were used without further purification. The purity of each reagent was verified before experiments using mass spectrometry. The glycolaldehyde sample was preheated to 330 K and dosed to the UHV system through a stainless steel dosing tube approximately 10 cm away from crystal surface. The furfural and acetaldehyde samples were dosed with the liquid samples at room temperature.

The TPD measurements were performed in a UHV chamber with a base pressure of 1×10^{-10} Torr, equipped with a mass spectrometer, an Auger electron spectrometer (AES), a sputter gun and an Fe source, as described previously [25]. A Ni(111) single crystal (Princeton Scientific, 99.99%, 2 mm thick and 10 mm in diameter) was placed at the center of the UHV chamber by directly spot-welding to two tantalum posts, allowing resistive heating and cooling with liquid nitrogen. A chromel–alumel K type thermocouple was welded onto the back of the Ni sample for temperature measurement. The Ni(111) surface was cleaned using cycles of sputtering in neon followed by annealing at 1100 K. Based on previous work using AES [26], LEED and STM [27], the growth of Fe on Ni(111) followed a layer-by-layer growth mechanism. The ML Fe/Ni(111) bimetallic surface was prepared using physical vapor deposition when the Ni(111) surface temperature was held at 300 K. The amount of Fe on the surface was controlled by the current of the Fe metal source and the deposition time. After deposition, the composition of the ML Fe/Ni(111) surface was estimated using the AES method described previously [28]. The relative Auger intensity ratio (I_{Fe}/I_{Ni}) for the ML Fe/Ni(111) surface is around 0.15 [29].

3. Results and discussion

3.1. DFT calculation results

DFT calculations were performed for the three types of biomass-derivatives, glycolaldehyde, acetaldehyde and furfural, on Ni(111) and ML Fe/Ni(111) surfaces. Fig. 1 shows the top and side views of the optimized adsorption configurations of the three molecules on the ML Fe/Ni(111) surface. The binding energies, as well as the bond lengths in glycolaldehyde, acetaldehyde and furfural in gas phase and adsorbed configurations on Ni(111) and ML Fe/Ni(111) surfaces are summarized in Table 1. Due to the complex structure, the carbon and oxygen atoms in furfural are numbered in the molecular structure shown in Table 1.

As shown in Fig. 1, glycolaldehyde is bonded onto the ML Fe/Ni(111) surface through both the C═O and C – O functional groups, leading to an increase in the C═O and C – O bond lengths in Table 1. The adsorption of acetaldehyde onto the ML Fe/Ni(111) surface is through the carbonyl group in an η2(C,O) configuration, which agrees well with the increase in the C═O bond length. Furfural adsorbs onto the ML Fe/Ni(111) surface through both the furan ring and the carbonyl group, consistent with the bond length increase in the corresponding functional groups after

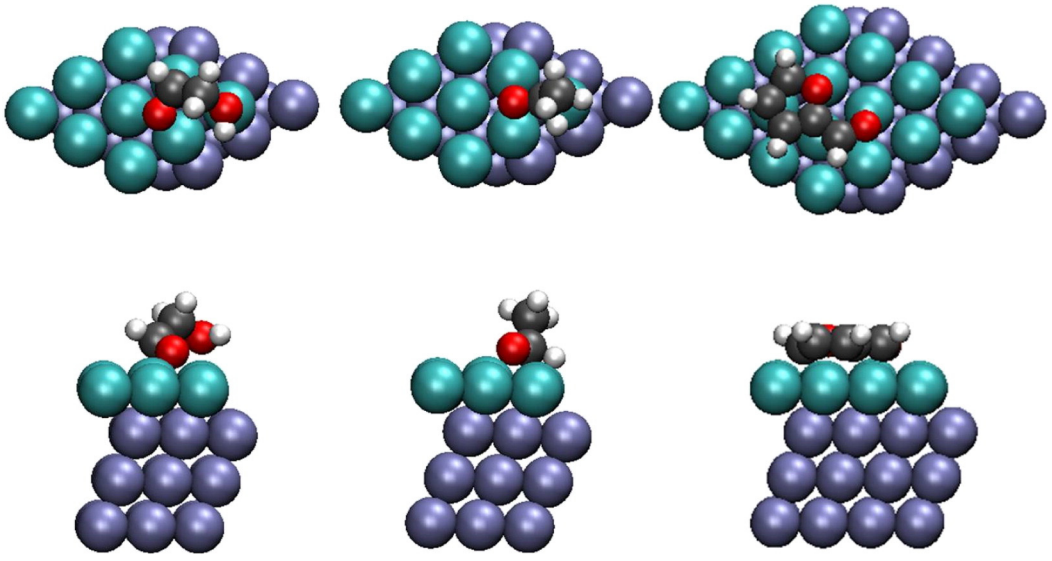

Fig. 1. Top and side views of the optimized configurations of glycolaldehyde, acetaldehyde and furfural on the ML Fe/Ni(111) surface (Ni: iceblue, Fe: aqua, C: gray, O: red, H: white). (For interpretation of the references to color in this figure legend, the reader is referred to the web version of this article.)

Please cite this article as: W. Yu, J.G. Chen, Reaction pathways of model compounds of biomass-derived oxygenates on Fe/Ni bimetallic surfaces, Surf. Sci. (2015), http://dx.doi.org/10.1016/j.susc.2015.01.009

Table 1
Surface d-band centers (eV) of Ni(111) and ML Fe/Ni(111) surfaces as well as the comparison of bond lengths (in Å) and binding energies (BE) (in kcal/mol) of glycolaldehyde, acetaldehyde and furfural in gas phase and adsorbed on corresponding surfaces.

		Gas phase	Ni(111)	ML Fe/Ni(111)
d-Band center		/	−1.37	−0.94
Glycolaldehyde	BE	/	−11.100	−27.500
	C═O	1.226	1.350	1.408
	C−O	1.401	1.448	1.453
	C−C	1.504	1.513	1.494
Acetaldehyde	BE	/	−5.861	−13.550
	C═O	1.220	1.325	1.354
	C−C	1.495	1.501	1.500
Furfural	BE	/	−20.337	−31.609
	C_1-O_1	1.229	1.320	1.340
	C_1-C_2	1.448	1.435	1.422
	C_2-C_3	1.382	1.433	1.430
	C_3-C_4	1.419	1.425	1.440
	C_4-C_5	1.373	1.449	1.449
	C_5-O_2	1.359	1.474	1.471
	O_2-C_2	1.378	1.409	1.414

adsorption. For example, compared with the gas phase, the bond lengths of C_1-O_1 in the carbonyl group and C_3-C_4 in the furan ring increase when furfural is adsorbed on the ML Fe/Ni(111) surface.

As shown in Table 1, for all three molecules, the binding energies are larger on the ML Fe/Ni(111) surface than clean Ni(111), indicating that the addition of the Fe layer binds the molecules more strongly. Furthermore, compared with those on Ni(111), the bond lengths in the molecules on the ML Fe/Ni(111) surface are generally longer due to the stronger interaction between the molecule and the surface. However, exceptions are found for the C−C bond lengths in glycolaldehyde and acetaldehyde as well as the C_1-C_2 bond length in furfural. The decrease in the C−C bond lengths in the three molecules on the ML Fe/Ni(111) surface can be correlated with the C−C bond scission activity, as discussed next.

3.2. TPD experiments of glycolaldehyde on Fe/Ni(111) surfaces

There are three possible net reaction pathways of glycolaldehyde: Eq. (1) the total decomposition pathway, Eq. (2) the reforming pathway and Eq. (3) the deoxygenation pathway.

$$a\ HOCH_2CHO \rightarrow 2a\ C_{ad} + 2a\ O_{ad} + 2a\ H_2 \quad \text{(Total decomposition)} \tag{1}$$

$$b\ HOCH_2CHO \rightarrow 2b\ CO + 2b\ H_2 \quad \text{(Reforming)} \tag{2}$$

$$c\ HOCH_2CHO \rightarrow c\ C_2H_4 + 2c\ O_{ad} \quad \text{(Deoxygenation)}. \tag{3}$$

Fig. 2 displays the TPD spectra of hydrogen (m/e = 2) and carbon monoxide (m/e = 28) from Ni(111) and ML Fe/Ni(111) surfaces after an exposure of 4 L glycolaldehyde. In Fig. 2a, the decomposition of glycolaldehyde leads to the desorption of H_2 at 345 K from the Ni(111) surface, as well as 340 K and 410 K from the ML Fe/Ni(111) surface. In Fig. 2b, the desorption peaks of the CO product are observed at 420 K from Ni(111) and 415 K from ML Fe/Ni(111). There is no desorption peak observed at m/e = 26 and m/e = 27 (not shown), indicating that the deoxygenation pathway to produce ethylene does not occur on Ni(111) or ML Fe/Ni(111). The chemisorbed glycolaldehyde on the two surfaces undergoes the total decomposition and reforming pathways.

The activities of glycolaldehyde following each reaction pathway on Ni(111) and ML Fe/Ni(111) surfaces are summarized in Table 2. The literature saturation coverages of H_2 (1 ML [30]) and CO (0.5 ML [31]) on Ni(111) were used for the quantification of the reaction pathways of glycolaldehyde as well as acetaldehyde and furfural discussed later. The details about the quantification method were described previously [2]. The Ni(111) surface shows a higher reforming activity (0.146) and total activity (0.193). Compared with the clean Ni(111) surface, the addition of Fe atoms on the surface leads to a decrease in the reforming activity, consistent with the shorter C−C bond length from the DFT results (Table 1).

3.3. TPD experiments of acetaldehyde on Fe/Ni(111) surfaces

As demonstrated in previous studies on the Ni/WC surface [32], possible net reaction pathways of acetaldehyde can be summarized as follows: Eq. (4) the total decomposition pathway, Eq. (5) the reforming pathway, Eq. (6) the deoxygenation reaction pathway and Eq. (7) the decarbonylation pathway.

$$a\,CH_3CHO \longrightarrow 2a\,C_{(ad)} + a\,O_{(ad)} + 2a\,H_2 \quad \text{(Total decomposition)} \tag{4}$$

$$b\,CH_3CHO \longrightarrow b\,CO + b\,C_{(ad)} + 2b\,H_2 \quad \text{(Reforming)} \tag{5}$$

$$c\,CH_3CHO \longrightarrow c\,C_2H_4 + c\,O_{(ad)} \quad \text{(Deoxygenation)} \tag{6}$$

$$d\,CH_3CHO \longrightarrow d\,CH_4 + d\,CO \quad \text{(Decarbonylation)}. \tag{7}$$

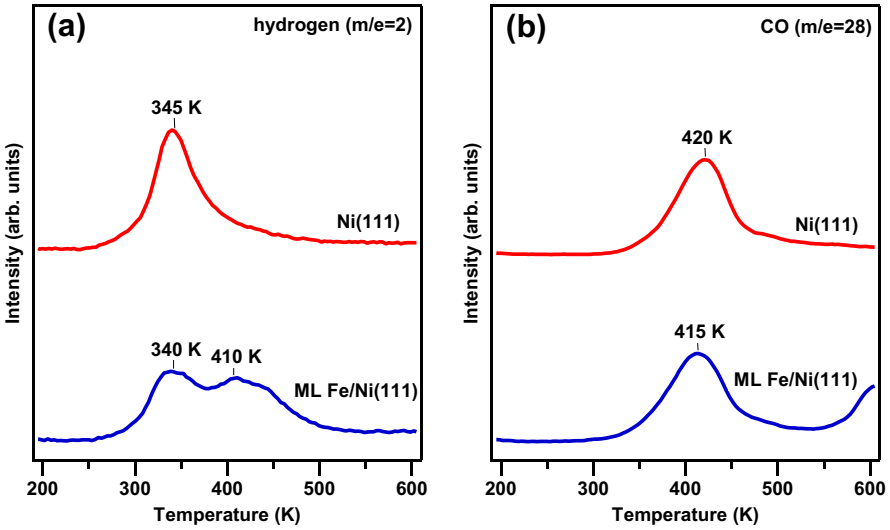

Fig. 2. TPD spectra of (a) hydrogen (m/e = 2) and (b) CO (m/e = 28) with an exposure of 4 L glycolaldehyde on Ni(111) and ML Fe/Ni(111) surfaces.

Please cite this article as: W. Yu, J.G. Chen, Reaction pathways of model compounds of biomass-derived oxygenates on Fe/Ni bimetallic surfaces, Surf. Sci. (2015), http://dx.doi.org/10.1016/j.susc.2015.01.009

Table 2
Reaction activities of glycolaldehyde, acetaldehyde and furfural on Ni(111) and ML Fe/Ni(111) surfaces from TPD measurements.

		Activity (monolayer per metal atom)				
		Decomposition	Reforming	Deoxygenation	Decarbonylation	Total activity
Glycolaldehyde	Ni(111)	0.047	0.146	–	–	0.193
	ML Fe/Ni(111)	0.033	0.116	–	–	0.149
Acetaldehyde	Ni(111)	0.005	0.157	–	–	0.162
	ML Fe/Ni(111)	0.000	0.104	–	–	0.104
Furfural	Ni(111)	0.079	0.071	0.000	0.003	0.153
	ML Fe/Ni(111)	0.007	0.027	0.003	0.000	0.037

Fig. 3 displays the TPD spectra of (a) H_2 and (b) CO after dosing 4 L acetaldehyde on Ni(111) and ML Fe/Ni(111) surfaces. Fig. 3a shows that H_2 is produced from the Ni(111) surface and the ML Fe/Ni(111) surface at 365 K and 390 K, with a broader hydrogen desorption peak being observed on ML Fe/Ni(111) than on Ni(111). In Fig. 3b, the CO product desorbs from the Ni(111) surface at 430 K and the ML Fe/Ni(111) surface at 415 K. The desorption peak of ethylene or methane is not observed (not shown).

The detection of the H_2 and CO products indicates that chemisorbed acetaldehyde follows the total decomposition and reforming pathways on Ni(111) and ML Fe/Ni(111) surfaces. As compared in the quantification results summarized in Table 2, the clean Ni(111) surface displays higher reforming activity (0.157) and total activity (0.162). The ML Fe/Ni(111) surface shows lower reforming activity for acetaldehyde, similar with the results of glycolaldehyde.

3.4. TPD experiments of furfural on Fe/Ni(111) surfaces

The mechanism of furfural reaction on hydrogen pre-dosed Fe/Ni(111) surfaces has been published previously [29]. The results of furfural on clean Ni(111) and ML Fe/Ni(111) surfaces are presented here to draw a comparison with C_2 oxygenates, glycolaldehyde and acetaldehyde. As summarized previously [29], there are five possible reaction pathways of furfural on Fe/Ni(111) surfaces: Eq. (8) total decomposition, Eq. (9) reforming, Eq. (10) deoxygenation, Eq. (11) decarbonylation to produce propylene and Eq. (12) hydrogenation. Reaction (10) is the desirable pathway to produce 2-methylfuran via C–O bond scission in the carbonyl group with the furan ring intact.

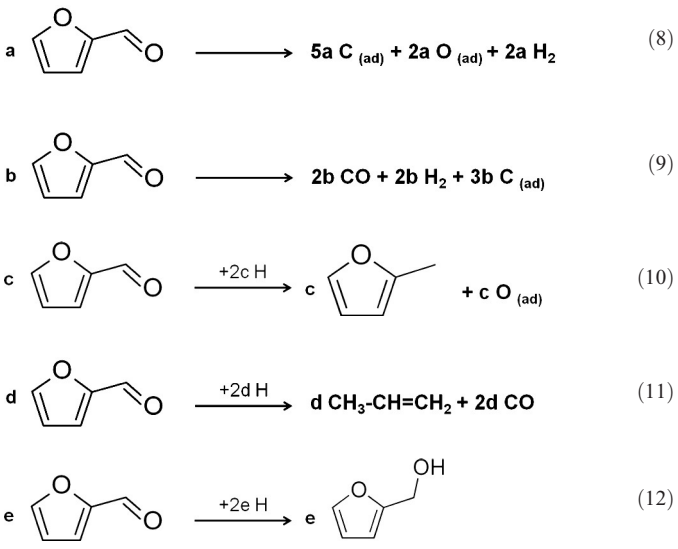

Fig. 4 compares the TPD spectra of (a) H_2, (b) CO, (c) propylene and (d) 2-methylfuran with an exposure of 4 L furfural on Ni(111) and ML Fe/Ni(111) surfaces. Furfuryl alcohol (m/e = 98) is not observed from the TPD spectra on either Ni(111) or ML Fe/Ni(111) (not shown here).

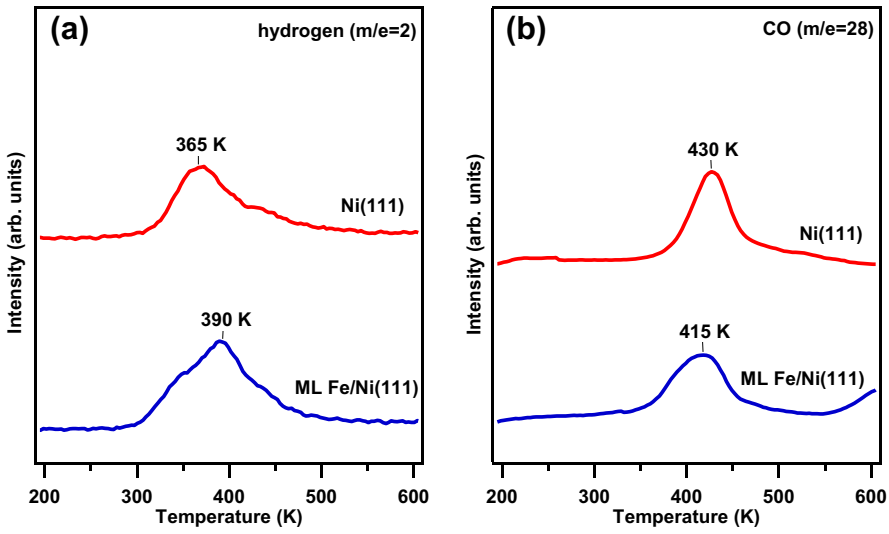

Fig. 3. TPD spectra of (a) hydrogen and (b) CO following 4 L acetaldehyde exposure on Ni(111) and ML Fe/Ni(111) surfaces.

Please cite this article as: W. Yu, J.G. Chen, Reaction pathways of model compounds of biomass-derived oxygenates on Fe/Ni bimetallic surfaces, Surf. Sci. (2015), http://dx.doi.org/10.1016/j.susc.2015.01.009

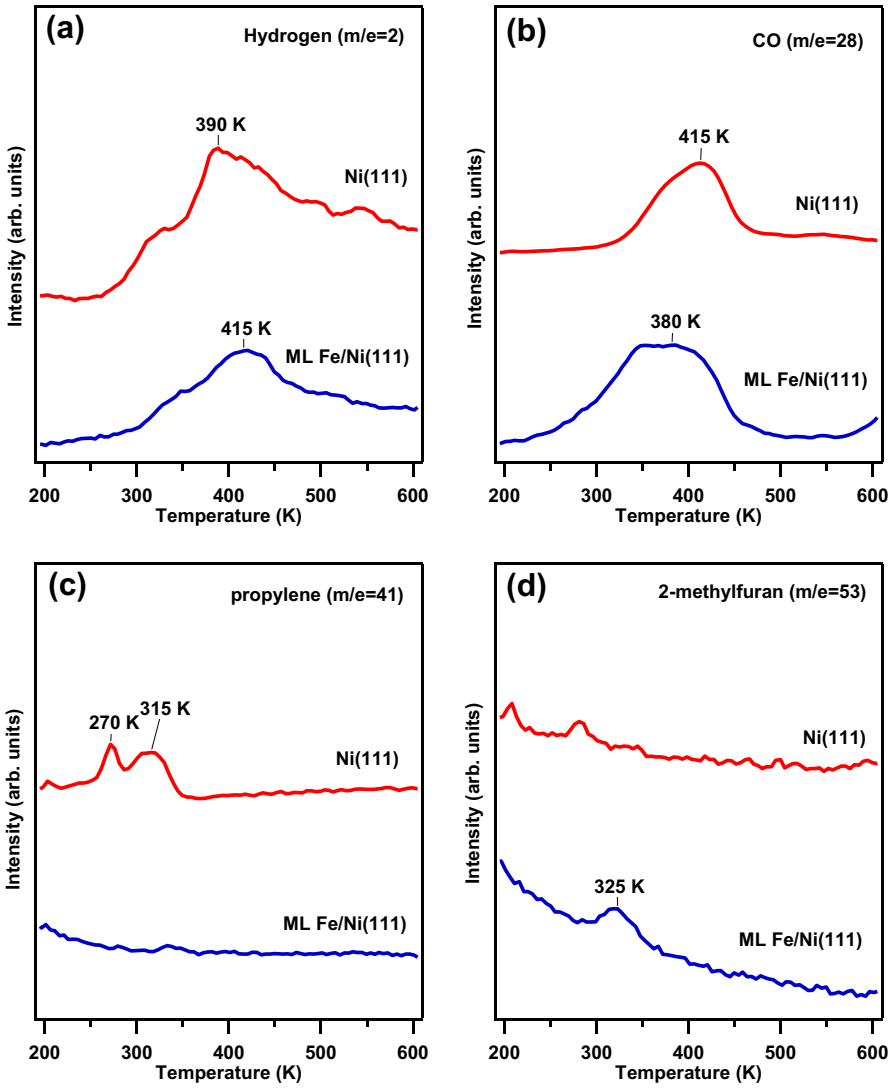

Fig. 4. TPD spectra of (a) hydrogen (m/e = 2), (b) CO (m/e = 28), (c) propylene (m/e = 41) and (d) 2-methylfuran (m/e = 53) with an exposure of 4 L furfural on Ni(111) and ML Fe/Ni(111) surfaces.

As shown in Fig. 4a, H_2 desorbs from Ni(111) at 390 K and from ML Fe/Ni(111) at 415 K. In Fig. 4b, the desorption peak of CO from furfural decomposition is observed at 415 K on Ni (111) and 380 K on ML Fe/Ni(111). Fig. 4c is the desorption profile of propylene, from the decarbonylation of furfural, at 270 K and 315 K from Ni(111). The desorption peak area of propylene from the ML Fe/Ni(111) surface is negligible. Fig. 4d shows the desorption of 2-methylfuran. The production of 2-methylfuran occurs at 325 K from the ML Fe/Ni(111) surface, but not from Ni(111), indicating that the addition of ML Fe on Ni(111) introduces the new deoxygenation pathway for 2-methylfuran production.

The amount of furfural following each reaction pathway is quantified and summarized in Table 2. The details about the quantification method was described previously [29]. On the Ni(111) surface, furfural shows a high reforming activity (0.071) and total activity (0.153). There is no 2-methylfuran production activity on the Ni(111) surface. With the addition of monolayer Fe on the surface, the reforming activity and total activity of furfural decrease to 0.027 and 0.037, respectively. Different from the Ni(111) surface, ML Fe/Ni(111) shows an activity of 0.003 for the desirable 2-methylfuran production.

3.5. Correlation between DFT and experimental results

It should be pointed out that a detailed comparison of the entire reaction network and activation barriers for the three molecules on Ni(111) and ML Fe/Ni(111) surfaces would be needed to directly correlate theoretical predictions with experimental results. However, these calculations would be computationally expensive, even for relatively small oxygenate molecules. The primary purpose of the current study is to use relatively simple calculations of binding energies and bond lengths of reactants and likely intermediates to help understand experimental results of reaction pathways.

As compared in Table 1, the binding energies of glycolaldehyde, acetaldehyde and furfural on the ML Fe/Ni(111) surface are stronger than those on Ni(111). The difference in the binding energies arises from the different electronic properties in the surfaces. The d-band density of states (DOS) for clean Ni(111) and ML Fe/Ni(111) surfaces are calculated and compared in Fig. 5. The DOS of the clean Ni(111) surface is relatively narrow. With the addition of an Fe layer on top of Ni(111), the distribution of the d-band states becomes wider. Based on the calculated d-band DOS results, the surface d-band centers for clean Ni(111) and ML Fe/Ni(111) surfaces are −1.37 eV and −0.94 eV,

Please cite this article as: W. Yu, J.G. Chen, Reaction pathways of model compounds of biomass-derived oxygenates on Fe/Ni bimetallic surfaces, Surf. Sci. (2015), http://dx.doi.org/10.1016/j.susc.2015.01.009

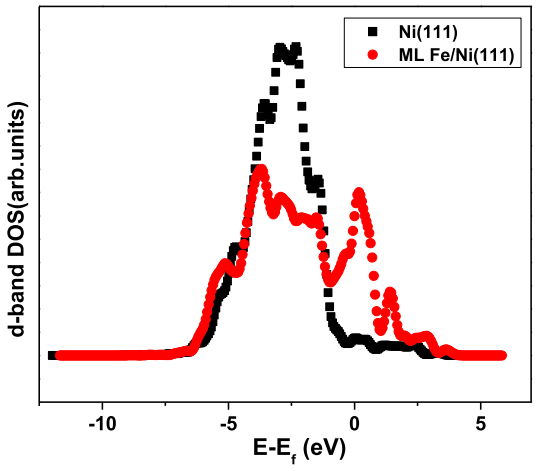

Fig. 5. DFT calculated d-band density of states for Ni(111) and ML Fe/Ni(111) surfaces.

respectively. With the addition of an Fe monolayer on the surface, the surface d-band center shifts closer to the Fermi level, leading to stronger binding energies of the three molecules on ML Fe/Ni(111).

There is a correlation between the adsorption geometry and the activity of the reforming pathway. Based on the TPD quantification results summarized in Table 2, Ni(111) shows higher reforming activity than the ML Fe/Ni(111) surface for all three molecules, indicating that the addition of the Fe monolayer reduces the reforming pathway that requires facile C – C bond cleavage. This is consistent with the DFT calculation results. As shown in Table 1, compared with the gas phase molecules, the C – C bond lengths increase when the molecules are adsorbed onto Ni(111) surface, especially for glycolaldehyde and acetaldehyde. The weakening of the C – C bond should contribute to the high reforming activity on Ni(111). On the other hand, due to the stronger binding between the molecules and the ML Fe/Ni(111) surface, the bond lengths in the molecules are generally longer than those on the Ni(111) surface, except for the C – C bond lengths. The C – C bond lengths in glycolaldehyde and acetaldehyde as well as the $C_1 - C_2$ bond length in furfural are shorter on ML Fe/Ni(111) than on the Ni(111) surface. The decrease in those C – C bond lengths leads to the suppression in reforming activity on the ML Fe/Ni(111) surface.

Based on the TPD results, on Ni(111) and ML Fe/Ni(111) surfaces, the adsorbed glycolaldehyde and acetaldehyde molecules mostly follow the reforming pathway to produce syngas. In comparison, as shown in Section 3.4, furfural mainly follows the reforming pathway on Ni(111). However, with the addition of Fe monolayer onto the surface, the reforming pathway is suppressed and the deoxygenation pathway for the desirable 2-methylfuran production is promoted. The detailed mechanism of furfural reaction on hydrogen-predosed ML Fe/Ni(111) surface has been shown in a previous study, with the increase in the deoxygenation pathway activity of furfural being attributed to the combination of lengthening in the C═O carbonyl bond and a slightly tilted furan ring away from the surface [29]. Similar factors might also contribute to the enhanced deoxygenation pathway in the current study, i.e., on Fe/Ni(111) without predosed hydrogen atoms.

4. Conclusions

In the current work, glycolaldehyde, acetaldehyde and furfural are studied on Ni(111) and ML Fe/Ni(111) surfaces as model compounds of the three classes of biomass, cellulose, hemicellulose and lignin. The ML Fe/Ni(111) surface is identified as a promising non-precious bimetallic surface for biomass conversion. The addition of Fe monolayer on the Ni(111) surface suppresses the reforming pathway due to a decrease in the C – C bond length. The Fe/Ni(111) surface also promotes the deoxygenation pathway of furfural resulting from the lengthening of the C – O bond of the carbonyl group.

Acknowledgment

This article was based on work supported as part of the Catalysis Center for Energy Innovation, an Energy Frontier Research Center funded by the U.S. Department of Energy, Office of Science,Office of Basic Energy Sciences under Award Number DE-SC0001004. Additionally, the DFT calculations in this work were performed using computational resources at Center for Functional Nanomaterials, Brookhaven National Laboratory, supported by the U.S. DOE/BES, under Contract No. DE-AC02-98CH10886.

Reference

[1] J.W. Medlin, ACS Catal. 1 (2011) 1284.
[2] W.T. Yu, M.A. Barteau, J.G. Chen, J. Am. Chem. Soc. 133 (2011) 20528.
[3] A.G. Gayubo, B. Valle, A.T. Aguayo, M. Olazar, J. Bilbao, J. Chem. Technol. Biotechnol. 85 (2010) 132.
[4] J.P. Lange, E. van der Heide, J. van Buijtenen, R. Price, ChemSusChem 5 (2012) 150.
[5] G. Melaet, W.T. Ralston, C.-S. Li, S. Alayoglu, K. An, N. Musselwhite, B. Kalkan, G.A. Somorjai, J. Am. Chem. Soc. 136 (2014) 2260.
[6] A.A. Gokhale, J.A. Dumesic, M. Mavrikakis, J. Am. Chem. Soc. 130 (2008) 1402.
[7] Q. Fu, H. Saltsburg, M. Flytzani-Stephanopoulos, Science 301 (2003) 935.
[8] Y.A. Ryndin, R.F. Hicks, A.T. Bell, Y.I. Yermakov, J. Catal. 70 (1981) 287.
[9] R.R. Davda, J.W. Shabaker, G.W. Huber, R.D. Cortright, J.A. Dumesic, Appl. Catal. B 43 (2003) 13.
[10] P.J. Berlowitz, D.W. Goodman, Surf. Sci. 187 (1987) 463.
[11] P.J. Berlowitz, J.E. Houston, J.M. White, D.W. Goodman, Surf. Sci. 205 (1988) 1.
[12] J.G. Chen, C.A. Menning, M.B. Zellner, Surf. Sci. Rep. 63 (2008) 201.
[13] D.W. Goodman, Ultramicroscopy 34 (1990) 1.
[14] J.A. Rodriguez, Surf. Sci. Rep. 24 (1996) 225.
[15] W.T. Yu, M.D. Porosoff, J.G. Chen, Chem. Rev. 112 (2012) 5780.
[16] J.R. Kitchin, N.A. Khan, M.A. Barteau, J.G. Chen, B. Yakshinksiy, T.E. Madey, Surf. Sci. 544 (2003) 295.
[17] S. Sitthisa, D.E. Resasco, Catal. Lett. 141 (2011) 784.
[18] S. Sitthisa, W. An, D.E. Resasco, J. Catal. 284 (2011) 90.
[19] G. Kresse, J. Furthmuller, Phys. Rev. B 54 (1996) 11169.
[20] G. Kresse, J. Hafner, Phys. Rev. B 47 (1993) 558.
[21] G. Kresse, J. Furthmuller, Comput. Mater. Sci. 6 (1996) 15.
[22] C.M. Ammann, G.A. Meehl, W.M. Washington, C.S. Zender, Geophys. Res. Lett. 30 (2003) 1657.
[23] J.P. Perdew, J.A. Chevary, S.H. Vosko, K.A. Jackson, M.R. Pederson, D.J. Singh, C. Fiolhais, Phys. Rev. B 46 (1992) 6671.
[24] M.P. Teter, M.C. Payne, D.C. Allan, Phys. Rev. B 40 (1989) 12255.
[25] M. Salciccioli, W. Yu, M.A. Barteau, J.G. Chen, D.G. Vlachos, J. Am. Chem. Soc. 133 (2011) 7996.
[26] M. Myint, Y. Yan, J.G. Chen, J. Phys. Chem. C 118 (2014) 11340.
[27] B. An, L. Zhang, S. Fukuyama, K. Yokogawa, Phys. Rev. B 79 (2009) 085406.
[28] P.J. Cumpson, M.P. Seah, Surf. Interface Anal. 25 (1997) 430.
[29] W. Yu, K. Xiong, N. Ji, M.D. Porosoff, J.G. Chen, J. Catal. 317 (2014) 253.
[30] A. Winkler, Fresenius J. Anal. Chem. 319 (1984) 635.
[31] F.P. Netzer, T.E. Madey, J. Chem. Phys. 76 (1982) 710.
[32] W.T. Yu, Z.J. Mellinger, M.A. Barteau, J.G. Chen, J. Phys. Chem. C 116 (2012) 5720.

Please cite this article as: W. Yu, J.G. Chen, Reaction pathways of model compounds of biomass-derived oxygenates on Fe/Ni bimetallic surfaces, Surf. Sci. (2015), http://dx.doi.org/10.1016/j.susc.2015.01.009